Current Biology 24, 2805–2811, December 1, 2014 ©2014 Elsevier Ltd All rights reserved http://dx.doi.org/10.1016/j.cub.2014.10.006

Report

Dopamine-Induced Dissociation of BOLD and Neural Activity in Macaque Visual Cortex

Daniel Zaldivar,[1,2,*] Alexander Rauch,[1,3] Kevin Whittingstall,[4] Nikos K. Logothetis,[1,5] and Jozien Goense[1,6,*]

[1]Max Planck Institute for Biological Cybernetics, Spemannstrasse 38, 72076 Tübingen, Germany

[2]IMPRS for Cognitive and Systems Neuroscience, University of Tübingen, Österbergstrasse 3, 72074 Tübingen, Germany

[3]University Hospital of Psychiatry, University of Bern, 3000 Bern, Switzerland

[4]Département de Radiologie Diagnostique 3001, Université de Sherbrooke, 12e Avenue Nord, Sherbrooke, QC J1H 5N4, Canada

[5]Division of Imaging Science and Biomedical Engineering, University of Manchester, Manchester M13 9PT, UK

[6]Institute of Neuroscience and Psychology, University of Glasgow, 58 Hillhead Street, Glasgow G12 8QB, UK

Summary

Neuromodulators determine how neural circuits process information during cognitive states such as wakefulness, attention, learning, and memory [1]. fMRI can provide insight into their function and dynamics, but their exact effect on BOLD responses remains unclear [2–4], limiting our ability to interpret the effects of changes in behavioral state using fMRI. Here, we investigated the effects of dopamine (DA) injections on neural responses and haemodynamic signals in macaque primary visual cortex (V1) using fMRI (7T) and intracortical electrophysiology. Aside from DA's involvement in diseases such as Parkinson's and schizophrenia, it also plays a role in visual perception [5–8]. We mimicked DAergic neuromodulation by systemic injection of L-DOPA and Carbidopa (LDC) or by local application of DA in V1 and found that systemic application of LDC increased the signal-to-noise ratio (SNR) and amplitude of the visually evoked neural responses in V1. However, visually induced BOLD responses decreased, whereas cerebral blood flow (CBF) responses increased. This dissociation of BOLD and CBF suggests that dopamine increases energy metabolism by a disproportionate amount relative to the CBF response, causing the reduced BOLD response. Local application of DA in V1 had no effect on neural activity, suggesting that the dopaminergic effects are mediated by long-range interactions. The combination of BOLD-based and CBF-based fMRI can provide a signature of dopaminergic neuromodulation, indicating that the application of multimodal methods can improve our ability to distinguish sensory processing from neuromodulatory effects.

Results

We combined fMRI with neurophysiology and pharmacology in five anesthetized nonhuman primates (*Macaca mulatta*), from which we acquired blood-oxygen-level-dependent (BOLD), functional cerebral blood flow (fCBF), and electrophysiology data while the animals viewed a rotating checkerboard stimulus. Figure 1A shows the experimental paradigm. We pharmacologically mimicked dopaminergic (DAergic) neurotransmission by systemic application of L-DOPA and Carbidopa (LDC). Carbidopa inhibits the breakdown of L-DOPA in the periphery, thereby preventing systemic changes in cerebral blood volume (CBV) that may affect the fMRI results (Figure S1 available online). The lack of systemic effects of the LDC injection is evidenced by the highly stable physiological parameters during and after injection (Table S1).

Evoked BOLD and Neural Responses under Systemic LDC

Figure 1B shows representative fMRI responses in primary visual cortex (V1) to visual stimulation. Figure 1C shows the changes in the BOLD response over the course of the LDC injection. BOLD modulation in the predrug period was 2.5% ± 1.1%, which is typical for anesthetized monkeys at 7T [9–11]. During the drug infusion, we observed a significant reduction in the visually induced modulation (Figures 1C and 1D; MOD_{drug} = 50% ± 5.3%; p = 0.034), which was sustained after the infusion was stopped (MOD_{post} = 60% ± 4.2%; p = 0.05). No significant changes in the baseline were found (Figure 1D).

We recorded local field potentials (LFPs) and multiunit spiking activity (MUA) to evaluate the effects of LDC application on neural activity. The power in the following three different frequency ranges was calculated: γ (40–150 Hz), MUA (900–3,000 Hz), and θ (4–8 Hz). γ and MUA ranges were most strongly correlated with the BOLD signal [2, 3, 12], whereas θ was used to indicate whether LDC affects the broadband-LFP power and to assess whether dopamine (DA) injection induces changes in the level of anesthesia. Figures 2A–2C show the average time course across experiments for the θ, γ, and MUA bands, respectively. LDC application resulted in an 18% increase in visual modulation in the γ band (Figure 2D; $MOD_{\gamma,drug}$ = 118% ± 4.2%; p = 0.024) and a 19% increase in the MUA band ($MOD_{MUA,drug}$ = 119% ± 5%; p = 0.031). The effect of LDC on the MUA amplitude reached baseline values ~4.5 min after the infusion was stopped. In contrast, for the γ band, the increase in visually induced modulation was long lasting and started to reduce ~12 min after the infusion was stopped. Additionally, we observed an increase in the signal-to-noise ratio (SNR) of the γ and MUA bands starting shortly after LDC injection (Figure 2E); the response to the stimulus increased, whereas the variability decreased (Figures 2B and 2C). The SNR in the γ band ($SNR_{\gamma,drug}$ = 13.7 dB ± 2.0 dB; p = 0.011) kept increasing after the infusion was stopped ($SNR_{\gamma,post}$ = 14.7 dB ± 2.0 dB; p = 0.012). The MUA band also showed an SNR increase after the start of the injection ($SNR_{MUA,drug}$ = 12.2 dB ± 2.2 dB; p = 0.012), which continued until the end of the trial ($SNR_{MUA,post}$ = 11.0 dB ± 2.0 dB; p = 0.026). In the θ band (Figure 2A), neither visually induced modulation nor SNR changed upon LDC infusion.

DA Effects Are Not Locally Induced in V1

We next investigated whether the increases in neural activity are locally induced in V1 or are due to a remote influence

*Correspondence: daniel.zaldivar@tuebingen.mpg.de (D.Z.), jozien.goense@glasgow.ac.uk (J.G.)

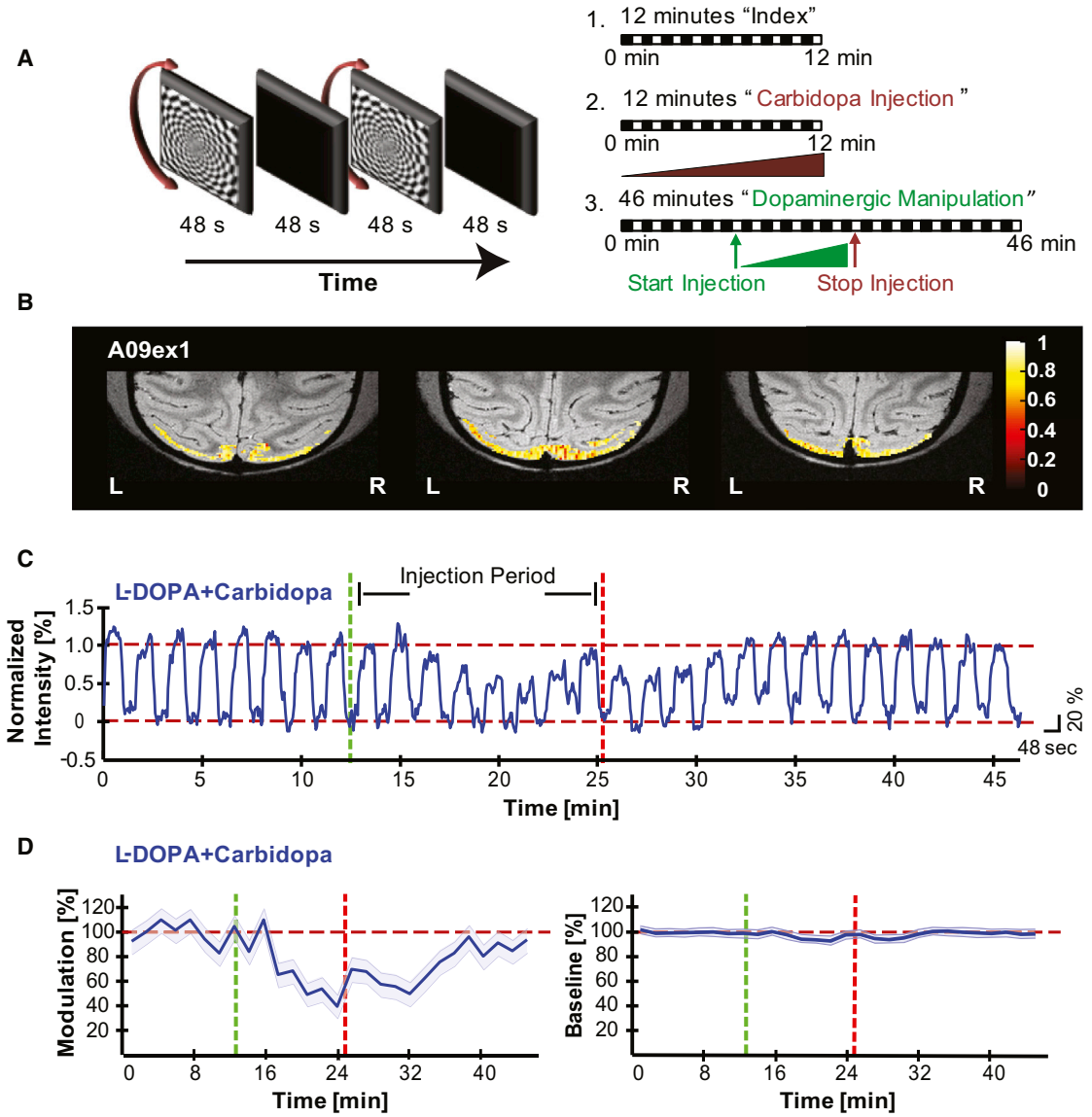

Figure 1. BOLD Responses under L-DOPA and Carbidopa Influence in Visual Cortex

(A) Experimental paradigm and design. The stimulus was a rotating checkerboard of 48 s followed by an isoluminant blank screen of 48 s (right). Every experiment was divided into three conditions: (1) a 12.8 min experiment without pharmacological manipulation, (2) a 12.8 min session with Carbidopa preconditioning (1.5 mg/kg diluted in 50 ml of PBS and injected at 1.1 ml/min), and (3) a 46 min session consisting of LDC manipulation (2.1 mg/kg + 0.5 mg/kg diluted in 50 ml of PBS and injected at 1.1 ml/min over a period of 12 min).

(B) Activation maps showing voxels with a significant response to the visual stimulus (eight-shot GE-EPI; FOV: 72 × 72 mm^2; TE/TR: 20/3,000 ms; flip angle 90°; matrix: 96 × 96), overlaid on an anatomical scan (FLASH), acquired at 7T with an in-plane resolution of 0.75 × 0.75 mm^2 and 2 mm slice thickness.

(C) The average BOLD time course (928 volumes) over 18 fMRI experimental sessions (five animals) shows a decrease in visually induced modulation by L-DOPA and Carbidopa; the green and the red lines show the start and stop of the L-DOPA-Carbidopa infusion.

(D) The average BOLD response to the visual stimulus (left), decreased by 50% compared to the predrug period, whereas the baseline did not change under L-DOPA and Carbidopa (right). The shaded areas represent the SE.

from other regions by injecting DA intracortically in V1 to determine whether this induces similar effects as systemic DA. Figures 3A–3C show the averaged traces of the θ, γ, and MUA bands during intracortical application of DA (5 mM) and show no discernible changes. Visually induced modulation in the γ and MUA bands (Figure 3D) was unchanged ($p = 0.23$). The SNR of the γ and MUA bands also remained unchanged during the experimental session (Figure 3E; $SNR_{\gamma,drug}$ = 9.0 dB ± 1.5 dB; $p = 0.31$; $SNR_{\gamma,post}$ = 8.8 dB ± 2.0 dB; $p = 0.13$; $SNR_{MUA,drug}$ = 10.1 dB ± 0.5 dB; $p = 0.18$; $SNR_{MUA,post}$ = 10.8 dB ± 2.0 dB; $p = 0.18$). Because different concentrations of DA can exert multiple modes of action [13], we tested whether different concentrations of intracortical DA affected the responses in V1. However, no concentration-dependent effects were observed (Figure S2).

The Effects of LDC on CBF Suggest an Increase in Energy Expenditure

Stimulus-induced increases in γ power and in MUA occurred simultaneously with a decrease in BOLD modulation. To

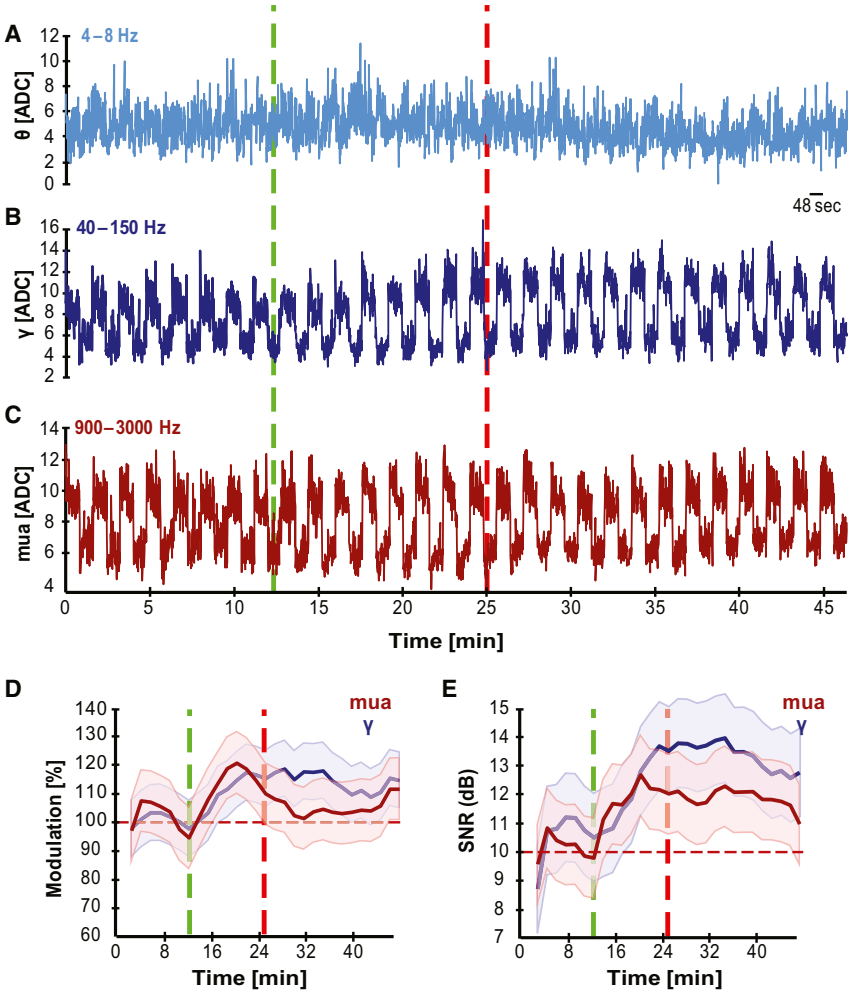

Figure 2. Systemic Application of L-DOPA and Carbidopa Increases Neural Responses in V1

Average time course of the neural activity (LFP and MUA bands) across experiments in response to L-DOPA and Carbidopa injection (n = 16).
(A) θ LFP band (4–8 Hz).
(B) γ LFP band (40–150 Hz).
(C) MUA band (900–3,000 Hz). The green and red lines denote the beginning and end of the systemic LDC infusion. In the MUA and γ bands, the amplitude of the visual response increased after LDC, whereas the variability of the baseline decreased.
(D) Percentage change in visual response of the γ band (blue) and MUA (red).
(E) The SNR of the γ band (blue) and the MUA (red) increased upon DA infusion. No changes were observed in the θ band.
The shaded areas represent the SE.

changes in the BOLD fMRI signal alone cannot be used to make inferences about increases or decreases in the underlying neural activity.

Neurophysiological Effects of DA Injection

Neurophysiological recordings under systemic LDC injection showed an increase in the amplitude and SNR of visually evoked responses. DA has been shown to improve the SNR in prefrontal cortex (PFC) and in sensory areas, including V1 [8, 14–16], thereby changing detection performance at the behavioral level [8, 16–18]. Increased neuronal activity in V1 has been shown to predict the timing of reward delivery, even when the cells were not driven by a visual stimulus [8, 18], highlighting the importance of DA for extracting behaviorally relevant information [17, 19].

However, local dopamine application did not change neural activity, in good agreement with the low density and sparse distribution of dopamine receptors (DARs) in V1 [20], suggesting that DA does not exert its effects on V1 itself. The increase in neural activity upon systemic DA may be mediated by long-range interactions from higher-order regions (e.g., frontal regions) [5, 15]. Large-scale interactions have been reported in other sensory modalities, including the visual, somatosensory, and auditory systems, suggesting that DA prepares the higher-order area for the processing of incoming sensory signals and promotes the readout of task-related information [14–16]. Manipulation of prefrontal D1 receptors increased the magnitude, reliability, and selectivity of neuronal responses in V4 [5], and similar mechanisms may play a role in V1.

The lack of DAergic effects upon local application is contrary to the inhibitory responses observed earlier [21, 22]. Although DA can exert different actions depending on concentration [13], none of the DA concentrations used in this study changed the amplitude or SNR of the visually evoked responses. Aside from species differences [20, 23], another possibility that could explain the differences is that the earlier experiments were performed with solutions in which the pH was not tightly controlled, whereas acidic pH depresses neuronal excitability [24].

resolve this potential discrepancy, we measured fCBF using arterial spin labeling (ASL). Figure 4A shows fCBF in early visual cortex, and Figure 4B shows the averaged time course of the CBF across experiments. There was a reliable, visually induced CBF modulation of 19% ± 7% during the predrug period, in agreement with earlier studies [11]. During the "drug" period, we observed an increase in modulation by 34% (MOD_{drug} = 134% ± 10%; p = 0.045). The maximum CBF increase of 43% was observed ~12 min after the infusion started and lasted ~20 min (MOD_{post} = 143% ± 10%; p = 0.034). We also observed significant increases in baseline CBF during and after the injection. An increase in the baseline was evident ~8 min after the start of the injection ($CBF_{baseline,drug}$ = 128% ± 5.2%; p = 0.022). The time course of the CBF changes upon LDC injection were similar to the time courses of the changes in the neuronal responses, suggesting that increases in neural activity may cause the CBF increases.

Discussion

Using BOLD-based and CBF-based fMRI combined with intracortical electrophysiology, we found that DAergic neuromodulation increased neural and CBF responses to a visual stimulus, whereas it decreased the BOLD response. Neuromodulators can exert strong influences on neural responses and alter neurovascular coupling [1, 3]. Our results show that

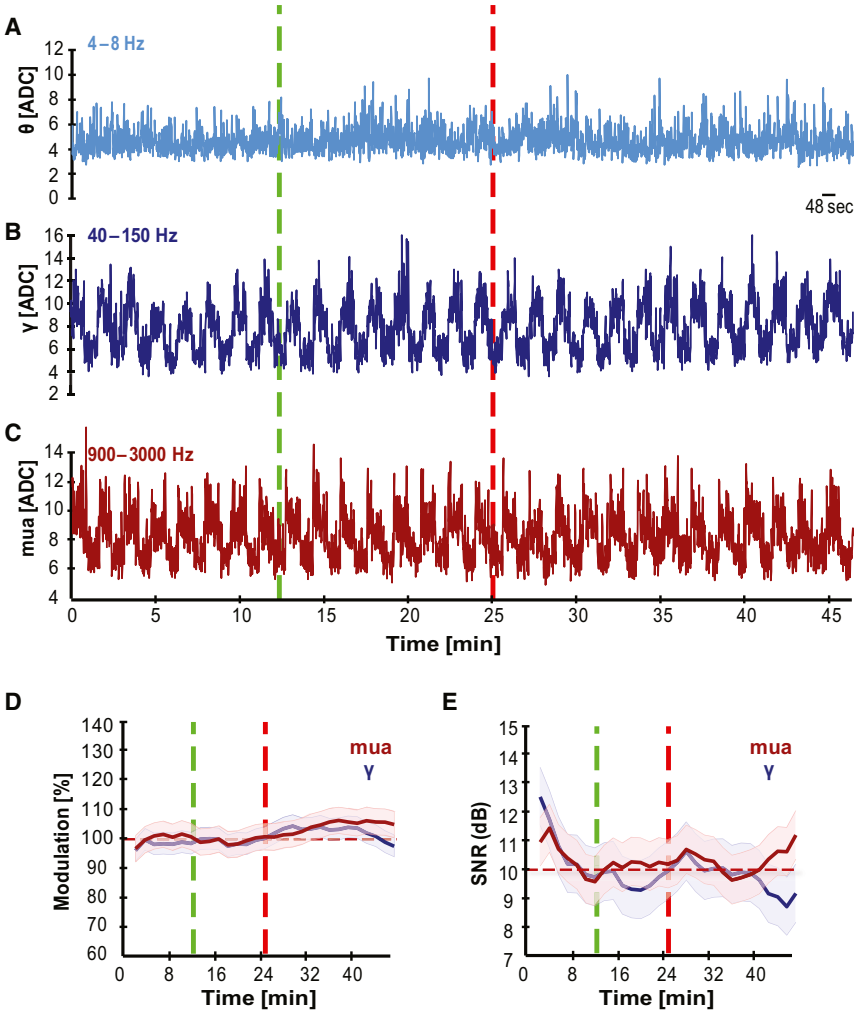

Figure 3. Local Application of DA Does Not Alter Neural Responses in V1

Average time course of the neural activity (LFP and MUA bands) across experiments, in response to local application of DA (n = 10; DA was diluted in artificial cerebrospinal fluid to a final concentration of 5 mM).
(A) θ LFP band (4–8 Hz).
(B) γ LFP band (40–150 Hz).
(C) MUA band (900–3,000 Hz). The green and red lines denote the beginning and end of the DA infusion. In the MUA and γ bands, the amplitude of the visual response was not affected by DA infusion.
(D) Percentage change in visual response of the γ (blue) band and MUA (red).
(E) The SNR of the γ band (blue) and the MUA (red) shows no changes upon DA. No changes were observed in the θ band.
The shaded areas represent the SE.

Functional Imaging

Our finding of a decrease in the evoked BOLD response and an increase in the CBF response upon systemic LDC injection extends previous observations in humans and macaques in which fMRI responses in V1 decreased with cues that predict and anticipate reward [6, 19]. A decrease in BOLD responses in V1 while behavioral performance improved after an acute dose of L-DOPA was seen in studies of amblyopia [7, 25]. However, BOLD increases have also been observed in humans in primary auditory and somatosensory cortex after DA agonist administration [26, 27]. These differences in BOLD responses upon DAergic neuromodulation can be partly explained by the difference in densities of DARs and DA innervation between cortical regions. DARs and DA innervations decrease along a rostral-caudal gradient, having the highest density in PFC and the lowest (or almost nonexistent) in occipital cortex [20]. Thus, BOLD responses to DAergic neuromodulation could differ in various sensory cortices because local influences of DA on the vasculature may modulate the blood supply [28, 29].

The effects of DA on the hemodynamic signals have been extensively addressed using different pharmacological agents in rats and monkeys [29–33]. For instance, amphetamines decreased CBV responses in occipital regions [33]. However, amphetamines are known to increase DA levels as well as alter the kinetics of other neurochemicals that affect the regional CBV [34], whereas CBV responses may differ from BOLD responses [35]. Different DARs exert different effects on the hemodynamic signals [30]; stimulation of D1 receptors (D1Rs) increases CBV and BOLD responses [30, 32], whereas blocking these receptors decreases them [30, 36]. The activation and deactivation of D2 receptors (D2Rs) produce opposite effects [37]. The present study did not consider receptor-specific responses but instead focused on understanding the balanced effects mediated by D1R and D2R interaction.

Neurovascular Coupling under Dopamine

Changes in the LFP are usually mirrored by changes in spiking and in the haemodynamic responses [3, 12]. Our observation of a dissociation between the BOLD and neurophysiological responses indicates that neurovascular coupling may differ under states of neuromodulation. Our results suggest that the increase in neural activity and CBF and the decrease in BOLD signal are caused by a disproportionate increase in O_2 consumption due to DAergic neuromodulation. The BOLD signal reflects the deoxyhemoglobin concentration (dHb concentration) and is affected by CBF, CBV, and the cerebral metabolic rate of oxygen consumption ($CMRO_2$). The stimulus-evoked BOLD decrease could be due to a CBF decrease or a dHb concentration increase after dopamine application. Because CBF increased, dHb production most likely also increased, i.e., an increase in $CMRO_2$. An increase in CBF modulation and a decrease in BOLD response can occur when the O_2 consumption increases by a proportionally larger amount than the inflow of fresh blood, leading to a relative increase in dHb concentration and a decrease in the BOLD signal compared to the preinjection response.

The increased neural activity also suggests a $CMRO_2$ increase because it has been shown that improving neurons' sensitivity is energetically draining [17, 38]. Autoradiography has also shown that the application of L-DOPA increases brain metabolism [39]. These observations are not surprising given that energy usage is tightly coupled to neural performance

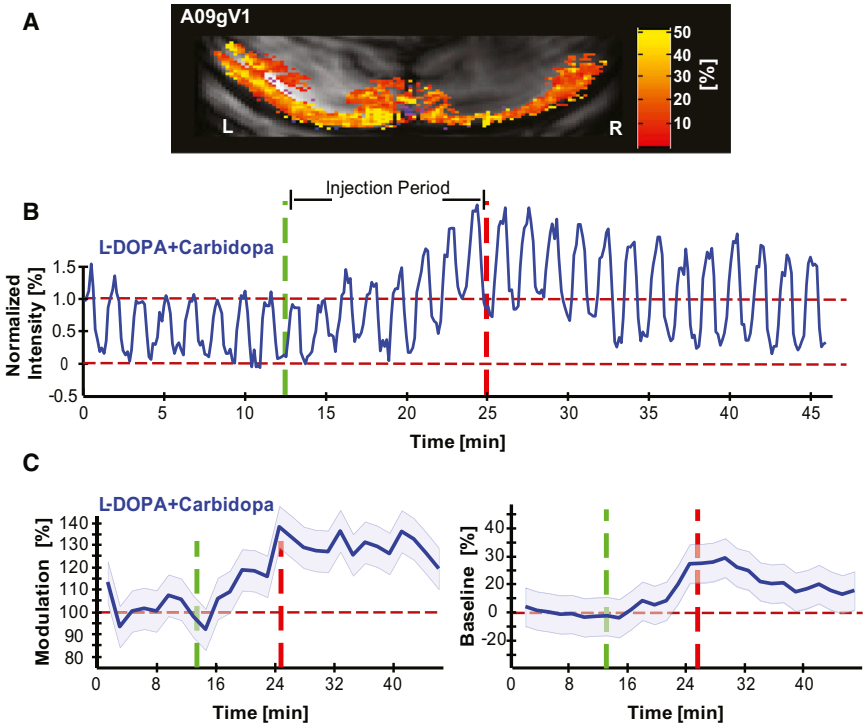

Figure 4. CBF Increases with L-DOPA and Carbidopa

(A) Activation patterns of functional CBF (using flow-sensitive alternating inversion recovery) in early visual cortex (monkey A09) in response to visual stimulation.

(B) The average time course over six CBF experimental sessions shows an increase in baseline-induced as well as visually induced CBF (six sessions acquired at 7T: TI, 1,400 ms; slab 6 mm; FOV, 5.5 × 2.4 mm^2; TE/TR, 9.5/4,500 ms; BW, 150 kHz, and one session acquired at 4.7T: TI, 1,400 ms; slab 6 mm; FOV, 6 × 3.2 mm^2; TE/TR, 9.1/4,500 ms; BW, 125 kHz).

(C) The average visually induced modulation increased by 43% (left) and the baseline changed by 31% (right) upon L-DOPA and Carbidopa infusion. The shaded areas represent the SE.

[3, 38]. The increase in CBF likely relates to neural activity because glucose metabolism, $CMRO_2$, and CBF are closely coupled [3, 40]. Increased neural activity in response to reward increases has been shown to increase the CBF [41].

The increased baseline CBF upon acute LDC injection commonly seen in humans and nonhuman primates [42–44] is usually attributed to vasodilation. However, the stimulus-induced CBF increases cannot be attributed to vasodilation alone. Vasodilation increases the baseline CBF and BOLD signals and reduces stimulus-evoked CBF and BOLD signals due to limited reserves, as seen in the case of hypercapnia (a potent vasodilator) [45, 46]. The possibility that the BOLD reduction is due to a ceiling effect, as seen in the case of hypercapnia or in pathology, is therefore unlikely because evoked CBF decreases in the case of vasodilation (e.g., in hypercapnia) or an inadequate CBF response [47].

Positron emission tomography studies have shown little or no change in $CMRO_2$ upon L-DOPA administration [43], the latter reflecting little or no change in baseline response, as was observed here. A lack of $CMRO_2$ increase, however, would not be able to explain our stimulus-driven results: comparing them again with hypercapnia, where $CMRO_2$ and neural activity do not change considerably, this would lead to very different CBF and BOLD responses to the stimulus than observed here [45]. Whether the increase in baseline CBF corresponds to an increase in metabolism cannot be deduced based on the current data. The baseline of the BOLD time course did not change, with a minor tendency to go down. It is possible that the increase in CBF is balanced out by an increase in dHb concentration in the baseline state, leading to little or no net baseline changes. Following the same reasoning as with the stimulus-induced responses, the small decrease in the baseline BOLD trace may indicate a small increase in $CMRO_2$ in the baseline condition as well. However, further study is needed to verify this.

The effects observed here are unlikely to be due to DA-induced changes in the level of anesthesia because no differences were observed in the θ band or the physiological parameters. The advantage of using anesthetized animals is that we could assess the effect of dopamine on neural and hemodynamic properties without needing to take behavioral parameters like attention, reward, and anticipation into account. Anesthetized animals also allow us to discriminate small changes because the anesthetized model allows for longer averaging times and higher SNR. However, differences in regional CBF under DAergic influence have been observed between awake and anesthetized animals [42], and differences may depend on the type of anesthesia. Because neuromodulatory properties strongly depend on the animal's behavioral state, including its level of alertness, this highlights the complexity of fMRI studies of neuromodulation, and it would be ideal to have a comparison of dopaminergic effects in awake and anesthetized animals.

The findings presented here provide us with a better understanding of the influence of neuromodulation on fMRI signals. The decrease of the BOLD signal in the face of increased energy use implies that the BOLD response may not always faithfully reflect the neural responses under neuromodulation and that caution is necessary in interpreting BOLD signals under neuromodulation. Combining BOLD measurements with CBF and/or CBV measurements can resolve these complexities and potentially provide a tool to discriminate sensory processing from neuromodulation. Such multidisciplinary approaches may improve the interpretation of fMRI studies where neuromodulation plays a role, for example, in studies of reward or attention, and also facilitate clinical applications of fMRI.

Experimental Procedures

fMRI and electrophysiology data were collected from six (four females) healthy rhesus monkeys (*Macaca mulatta*; 5–11 kg, 6–12 years old). All experimental procedures were carried out under approval of the local authorities (Regierungspräsidium, Baden-Württemberg, Tübingen, Germany, Project KY4/09) and were in full compliance with the guidelines of the European Community (EUVD 86/609/EEC).

Supplemental Information

Supplemental Information includes Supplemental Results, Supplemental Experimental Procedures, two figures, and one table and can be found with this article online at http://dx.doi.org/10.1016/j.cub.2014.10.006.

Acknowledgments

We thank Thomas Steudel, Mirko Linding, and Deniz Ipek for valuable technical support and Hellmut Merkle for designing and building the RF coils. We thank Veronika von Pföstl, Cesare Magri, and Almut Schüz for their support. Raymundo Baez-Mendoza and Yusuke Murayama provided comments on an earlier version of the manuscript. This work was supported by the Max Planck Society.

Received: September 30, 2014
Revised: September 30, 2014
Accepted: October 3, 2014
Published: November 20, 2014

References

1. Dayan, P. (2012). Twenty-five lessons from computational neuromodulation. Neuron *76*, 240–256.
2. Rauch, A., Rainer, G., and Logothetis, N.K. (2008). The effect of a serotonin-induced dissociation between spiking and perisynaptic activity on BOLD functional MRI. Proc. Natl. Acad. Sci. USA *105*, 6759–6764.
3. Logothetis, N.K. (2008). What we can do and what we cannot do with fMRI. Nature *453*, 869–878.
4. Sirotin, Y.B., and Das, A. (2009). Anticipatory haemodynamic signals in sensory cortex not predicted by local neuronal activity. Nature *457*, 475–479.
5. Noudoost, B., and Moore, T. (2011). Control of visual cortical signals by prefrontal dopamine. Nature *474*, 372–375.
6. Arsenault, J.T., Nelissen, K., Jarraya, B., and Vanduffel, W. (2013). Dopaminergic reward signals selectively decrease fMRI activity in primate visual cortex. Neuron *77*, 1174–1186.
7. Rogers, G.L. (2003). Functional magnetic resonance imaging (fMRI) and effects of L-dopa on visual function in normal and amblyopic subjects. Trans. Am. Ophthalmol. Soc. *101*, 401–415.
8. Shuler, M.G., and Bear, M.F. (2006). Reward timing in the primary visual cortex. Science *311*, 1606–1609.
9. von Pföstl, V., Li, J., Zaldivar, D., Goense, J., Zhang, X., Serr, N., Logothetis, N.K., and Rauch, A. (2012). Effects of lactate on the early visual cortex of non-human primates, investigated by pharmaco-MRI and neurochemical analysis. Neuroimage *61*, 98–105.
10. Goense, J., Logothetis, N.K., and Merkle, H. (2010). Flexible, phase-matched, linear receive arrays for high-field MRI in monkeys. Magn. Reson. Imaging *28*, 1183–1191.
11. Zappe, A.C., Pfeuffer, J., Merkle, H., Logothetis, N.K., and Goense, J.B. (2008). The effect of labeling parameters on perfusion-based fMRI in nonhuman primates. J. Cereb. Blood Flow Metab. *28*, 640–652.
12. Goense, J.B., and Logothetis, N.K. (2008). Neurophysiology of the BOLD fMRI signal in awake monkeys. Curr. Biol. *18*, 631–640.
13. Seamans, J.K., and Yang, C.R. (2004). The principal features and mechanisms of dopamine modulation in the prefrontal cortex. Prog. Neurobiol. *74*, 1–58.
14. Happel, M.F., Deliano, M., Handschuh, J., and Ohl, F.W. (2014). Dopamine-modulated recurrent corticoefferent feedback in primary sensory cortex promotes detection of behaviorally relevant stimuli. J. Neurosci. *34*, 1234–1247.
15. Jacob, S.N., Ott, T., and Nieder, A. (2013). Dopamine regulates two classes of primate prefrontal neurons that represent sensory signals. J. Neurosci. *33*, 13724–13734.
16. de Lafuente, V., and Romo, R. (2011). Dopamine neurons code subjective sensory experience and uncertainty of perceptual decisions. Proc. Natl. Acad. Sci. USA *108*, 19767–19771.
17. Servan-Schreiber, D., Printz, H., and Cohen, J.D. (1990). A network model of catecholamine effects: gain, signal-to-noise ratio, and behavior. Science *249*, 892–895.
18. Stănişor, L., van der Togt, C., Pennartz, C.M., and Roelfsema, P.R. (2013). A unified selection signal for attention and reward in primary visual cortex. Proc. Natl. Acad. Sci. USA *110*, 9136–9141.
19. Serences, J.T. (2008). Value-based modulations in human visual cortex. Neuron *60*, 1169–1181.
20. Lidow, M.S., Goldman-Rakic, P.S., Gallager, D.W., and Rakic, P. (1991). Distribution of dopaminergic receptors in the primate cerebral cortex: quantitative autoradiographic analysis using [3H]raclopride, [3H]spiperone and [3H]SCH23390. Neuroscience *40*, 657–671.
21. Gottberg, E., Montreuil, B., and Reader, T.A. (1988). Acute effects of lithium on dopaminergic responses: iontophoretic studies in the rat visual cortex. Synapse *2*, 442–449.
22. Reader, T.A. (1978). The effects of dopamine, noradrenaline and serotonin in the visual cortex of the cat. Experientia *34*, 1586–1588.
23. Phillipson, O.T., Kilpatrick, I.C., and Jones, M.W. (1987). Dopaminergic innervation of the primary visual cortex in the rat, and some correlations with human cortex. Brain Res. Bull. *18*, 621–633.
24. Tombaugh, G.C., and Somjen, G.G. (1996). Effects of extracellular pH on voltage-gated Na+, K+ and Ca2+ currents in isolated rat CA1 neurons. J. Physiol. *493*, 719–732.
25. Algaze, A., Leguire, L.E., Roberts, C., Ibinson, J.W., Lewis, J.R., and Rogers, G. (2005). The effects of L-dopa on the functional magnetic resonance imaging response of patients with amblyopia: a pilot study. J. AAPOS *9*, 216–223.
26. Weis, T., Puschmann, S., Brechmann, A., and Thiel, C.M. (2012). Effects of L-dopa during auditory instrumental learning in humans. PLoS ONE *7*, e52504.
27. Pleger, B., Blankenburg, F., Ruff, C.C., Driver, J., and Dolan, R.J. (2008). Reward facilitates tactile judgments and modulates hemodynamic responses in human primary somatosensory cortex. J. Neurosci. *28*, 8161–8168.
28. Krimer, L.S., Muly, E.C., 3rd, Williams, G.V., and Goldman-Rakic, P.S. (1998). Dopaminergic regulation of cerebral cortical microcirculation. Nat. Neurosci. *1*, 286–289.
29. Mandeville, J.B., Jenkins, B.G., Kosofsky, B.E., Moskowitz, M.A., Rosen, B.R., and Marota, J.J. (2001). Regional sensitivity and coupling of BOLD and CBV changes during stimulation of rat brain. Magn. Reson. Med. *45*, 443–447.
30. Mandeville, J.B., Sander, C.Y., Jenkins, B.G., Hooker, J.M., Catana, C., Vanduffel, W., Alpert, N.M., Rosen, B.R., and Normandin, M.D. (2013). A receptor-based model for dopamine-induced fMRI signal. Neuroimage *75*, 46–57.
31. Esaki, T., Itoh, Y., Shimoji, K., Cook, M., Jehle, J., and Sokoloff, L. (2002). Effects of dopamine receptor blockade on cerebral blood flow response to somatosensory stimulation in the unanesthetized rat. J. Pharmacol. Exp. Ther. *303*, 497–502.
32. Delfino, M., Kalisch, R., Czisch, M., Larramendy, C., Ricatti, J., Taravini, I.R., Trenkwalder, C., Murer, M.G., Auer, D.P., and Gershanik, O.S. (2007). Mapping the effects of three dopamine agonists with different dyskinetogenic potential and receptor selectivity using pharmacological functional magnetic resonance imaging. Neuropsychopharmacology *32*, 1911–1921.
33. Jenkins, B.G., Sanchez-Pernaute, R., Brownell, A.L., Chen, Y.C., and Isacson, O. (2004). Mapping dopamine function in primates using pharmacologic magnetic resonance imaging. J. Neurosci. *24*, 9553–9560.
34. Leonard, B.E., and Shallice, S.A. (1971). Some neurochemical effects of amphetamine, methylamphetamine and p-bromomethylamphetamine in the rat. Br. J. Pharmacol. *41*, 198–212.
35. Goense, J., Merkle, H., and Logothetis, N.K. (2012). High-resolution fMRI reveals laminar differences in neurovascular coupling between positive and negative BOLD responses. Neuron *76*, 629–639.
36. Choi, J.K., Mandeville, J.B., Chen, Y.I., Grundt, P., Sarkar, S.K., Newman, A.H., and Jenkins, B.G. (2010). Imaging brain regional and cortical laminar effects of selective D3 agonists and antagonists. Psychopharmacology (Berl.) *212*, 59–72.
37. Choi, J.K., Chen, Y.I., Hamel, E., and Jenkins, B.G. (2006). Brain hemodynamic changes mediated by dopamine receptors: Role of the cerebral microvasculature in dopamine-mediated neurovascular coupling. Neuroimage *30*, 700–712.
38. Laughlin, S.B., de Ruyter van Steveninck, R.R., and Anderson, J.C. (1998). The metabolic cost of neural information. Nat. Neurosci. *1*, 36–41.
39. Porrino, L.J., Burns, R.S., Crane, A.M., Palombo, E., Kopin, I.J., and Sokoloff, L. (1987). Local cerebral metabolic effects of L-dopa therapy in 1-methyl-4-phenyl-1,2,3,6-tetrahydropyridine-induced parkinsonism in monkeys. Proc. Natl. Acad. Sci. USA *84*, 5995–5999.

40. Kim, S.G., and Ogawa, S. (2012). Biophysical and physiological origins of blood oxygenation level-dependent fMRI signals. J. Cereb. Blood Flow Metab. *32*, 1188–1206.
41. Obayashi, S., Nagai, Y., Suhara, T., Okauchi, T., Inaji, M., Iriki, A., and Maeda, J. (2009). Monkey brain activity modulated by reward preferences: a positron emission tomography study. Neurosci. Res. *64*, 421–428.
42. Hershey, T., Black, K.J., Carl, J.L., and Perlmutter, J.S. (2000). Dopa-induced blood flow responses in nonhuman primates. Exp. Neurol. *166*, 342–349.
43. Leenders, K.L., Wolfson, L., Gibbs, J.M., Wise, R.J., Causon, R., Jones, T., and Legg, N.J. (1985). The effects of L-DOPA on regional cerebral blood flow and oxygen metabolism in patients with Parkinson's disease. Brain *108*, 171–191.
44. Montastruc, J.L., Celsis, P., Agniel, A., Demonet, J.F., Doyon, B., Puel, M., Marc-Vergnes, J.P., and Rascol, A. (1987). Levodopa-induced regional cerebral blood flow changes in normal volunteers and patients with Parkinson's disease. Lack of correlation with clinical or neuropsychological improvements. Mov. Disord. *2*, 279–289.
45. Zappe, A.C., Uludağ, K., and Logothetis, N.K. (2008). Direct measurement of oxygen extraction with fMRI using 6% CO2 inhalation. Magn. Reson. Imaging *26*, 961–967.
46. Sicard, K.M., and Duong, T.Q. (2005). Effects of hypoxia, hyperoxia, and hypercapnia on baseline and stimulus-evoked BOLD, CBF, and CMRO2 in spontaneously breathing animals. Neuroimage *25*, 850–858.
47. Blicher, J.U., Stagg, C.J., O'Shea, J., Østergaard, L., MacIntosh, B.J., Johansen-Berg, H., Jezzard, P., and Donahue, M.J. (2012). Visualization of altered neurovascular coupling in chronic stroke patients using multimodal functional MRI. J. Cereb. Blood Flow Metab. *32*, 2044–2054.